



Universiteit  
Leiden  
The Netherlands

## **Molecular electronics: controlled manipulation, noise and graphene architecture**

Tewari, S.

### **Citation**

Tewari, S. (2018, March 27). *Molecular electronics: controlled manipulation, noise and graphene architecture*. Casimir Research School, Delft. Retrieved from <https://hdl.handle.net/1887/58611>

Version: Not Applicable (or Unknown)

License: [Licence agreement concerning inclusion of doctoral thesis in the Institutional Repository of the University of Leiden](#)

Downloaded from: <https://hdl.handle.net/1887/58611>

**Note:** To cite this publication please use the final published version (if applicable).

Cover Page



Universiteit Leiden



The following handle holds various files of this Leiden University dissertation:

<http://hdl.handle.net/1887/58611>

**Author:** Tewari, S.

**Title:** Molecular electronics: controlled manipulation, noise and graphene architecture

**Issue Date:** 2018-03-27

## 7. Graphene based circuit

*Use of graphene as an electrode for molecular electronics has several benefits. Foremost is the stability of the graphene lattice at room temperature which could help in making stable room temperature devices. Second thanks to its two-dimensional structure, it provides the possibility to modify and image its atomic structure. The electroburning technique used widely to make graphene nanogaps does not provide the control needed for proper characterization of the gap and its scalability to multiple electrode circuits. First, in this chapter an overview of previous work on graphene based electrodes, their achievements and limitations is presented. Followed by this a discussion of our results on exploring more direct cutting methods for making graphene nanogaps is presented. Specially, the STM tip based cutting which can provide controlled cuts up to 1.6 nm gap size.*

The work is done in collaboration with - Kim Akius<sup>1</sup>, Gaurav Nanda<sup>2</sup> and Jan M. van Ruitenbeek<sup>1</sup>

<sup>1</sup>Huygens-Kamerlingh Onnes Laboratorium, Universiteit Leiden, The Netherlands.

<sup>2</sup>Kavli Nanolab, TU Delft, The Netherlands.

## 7.1 Introduction

Silicon technology has a monopoly in electronics industry from the time the transistor was invented. The main reason behind it is the continuous development of lithographic techniques using excimer lasers like krypton fluoride (248 nm), then argon fluoride or deep ultra-violet (193 nm) and now extreme ultra-violet or EUV (13.5 nm). This allowed the silicon industry to reduce the size of the transistor from 800 nm in 1990 to 10 nm in 2016<sup>1</sup>. When the size of the transistors became smaller than 50 nm, problems started to appear. The leakage current between the source and drain terminals of the transistors even in an OFF state became comparable to the ON state current which has been reduced due to the small size of the gate electrode and thus small area of the inversion layer which is responsible for charge transport in the ON state. A workaround to this problem was brought by the use of finFET technology which increased the inversion layer area and thus increased the ON state current further. Another big issue at the moment is due to the large density of these transistors in a chip<sup>2</sup>, because of which a large amount of heat is generated which ought to be removed. Silicon industry is continuously coming up with better architectures of transistors so that they can reduce their size further and could thus keep the Moore's law going. Recently, in June 2017 Intel showcased a 5 nm size transistor using their latest transistor architecture called GAAFET (gate all around FET). They claim that they can reach with the same architecture down to 3 nm.

The obvious question one can ask is how much smaller these transistors can be made under silicon technology and what will be next? We don't know the answer to this yet but possible paths could be: just 3D stacking of many logic dies, use of other III-V materials, carbon (graphene and nanotubes) and or use of individual molecules as electronic components. Regarding lithography techniques, the latest EUV lithography can lead the path forward. Electron beam lithography (EBL), has a higher resolution but is not favoured so far for large throughput work, due to its much larger writing times. Recent developments in EBL like using multi-column and multiple beam solutions<sup>3</sup> has reduced the EBL writing time and could thus also form a possible choice in lithography.

One may raise the question whether there is even a benefit of going further smaller in size using silicon. The next dimension scale that is waiting is the fundamental dimension limit formed by the basic constituents of matter like single molecules and single atoms. Study of organic molecules as electronic components has been an extensive field of research in itself since nearly 45 years, under the name of molecular electronics. A decade or two ago when silicon electronics was still operating in the size range of 100's of nanometers, molecular electronics showed a possibility of large benefits in dimension scaling on using single molecules. But today when silicon technology is standing already at the doorstep with transistors in the size scale of 5-10 nm, what does molecular electronics have to offer?

Molecules do have enough to offer! Molecular electronics is not only about scaling but also about functionalities. A silicon-based transistor however small it becomes is just a classical switch and an amplifier. Since the time of its invention what it does is controlling the current flowing between a source and a drain terminal by modifying

---

<sup>1</sup> These dimensions quoted are typically the channel length in the transistor.

<sup>2</sup> For example-there are around 3.3 billion transistors in each Apple A10 chip of 125 mm<sup>2</sup> area.

<sup>3</sup> This comes with the name of electron-beam direct-write (EbDW) technologies.

## 7.2 Graphene vs metallic electrodes

---

the voltage applied to the gate terminal. Single-molecule devices, on the other hand, can make use of the quantum mechanical properties<sup>4</sup> of individual electrons and provide various functionalities like quantum interference, spin selection or filtering, Coulomb blockade, electron-phonon interaction, thermoelectricity and much more. Desai *et al.*<sup>[1]</sup> have recently demonstrated a MoS<sub>2</sub> transistor with 1 nm gate length using a single-walled carbon nanotube as a gate electrode. Another new method picking up the reputation for making controlled nanoscale patterns other than usual lithographic techniques is directed self-assembly (DSA) of block copolymers<sup>[2]</sup>. Self-assembly of molecular circuits has been studied extensively, but these self-assembled structures are randomly distributed over large length scales. Using DSA, it has been shown that the growth of these self-assemblies can be controlled to make desired nanoscale patterns at much faster rate.

On the other hand it has to be noted that most of the molecular electronics research is done on platforms which are not scalable. By scalable I mean that in most of the measurement setups (like mechanically controlled break junction and STM break junctions) we can study single-molecules, but it is not possible to extend this to a multi-molecular circuit. Electro-migration based junctions are mostly fabricated with many junctions on the same chip, but due to the statistical nature of electro-migration, the location and width of these junction gaps are not very controlled, scaling of these to a multi-molecular circuit or even to multi-terminal devices is very challenging. Electro-migration junctions can be fabricated in thin metallic strips (mostly gold) and two-dimensional conducting materials like graphene<sup>5</sup>.

We have used graphene as our material for making electrodes keeping in mind both controlled measurements for single molecules and possible scalability of the system. For these goals, we have decided to study other approaches to make nanogaps for connecting single molecules. In the coming sections, we will first discuss the choice of system and the approach we took and then we will present our findings.

## 7.2 Graphene vs metallic electrodes

There are certain advantages and disadvantages of both graphene and metallic electrodes. Metallic electrodes like gold electrodes have been used extensively for studying single molecules electronic transport due to their chemical inertness to impurities. Gold binds very strongly to sulphur and nitrogen atoms which makes thiols (-SH) and amines (-NH) popular as anchoring groups for attaching molecules chemically between two Au leads. In contrast, using graphene as electrodes for molecular electronics is rather new<sup>[3]</sup> and freshly exposed graphene edges during nanogap formation are very reactive and thus are prone to accumulate dirt on the edges. The

---

<sup>4</sup> Even in silicon-based devices the bulk band structure is defined by quantum mechanics and at small length scales quantum tunneling of electrons starts to cause increase in leakage current.

<sup>5</sup> In graphene, it is technically electroburning not electromigration

[1] Sujay B. Desai et al. In: *Science* 354 (2016), p. 99.

[2] Jeong Gon Son et al. In: *Advanced Materials* 25 (2013), p. 4723.

[3] Ferry Prins et al. In: *Nano Letters* 11 (2011), p. 4607.

anchoring groups, in this case, are mostly  $\pi$ -conjugated systems<sup>[3,4]</sup>, fullerene<sup>[5]</sup> and amine groups<sup>[6,7]</sup>. Graphene electrodes are more stable in comparison to metallic electrodes, even at room temperature due to the reduced mobility of carbon atoms connected with  $sp^2$  carbon bonds. The downside of graphene is that the mobility of electrons in graphene decreases dramatically with increasing concentration of defects<sup>[8,9]</sup>. Another benefit of metal electrodes is that the metallic bonds allow for repeated fusion and breaking of atomic-size contacts, in STM or MCBJ type of instruments.

Graphene-based single-molecule devices are predicted to have good thermoelectric properties<sup>[10]</sup>. Recent experiments<sup>[11]</sup> have shown that by careful tuning of molecular resonances large thermoelectric power factors can be achieved in such systems. Physisorbed molecular wires on graphene electrodes are predicted<sup>[12]</sup> to have a universal behaviour regarding the position of transmission resonances. This means that for various binding locations of the molecule with respect to the electrodes, the positions of transmission resonances with respect to Fermi energy remain intact, which is not expected for 3D metallic electrodes.

Out of all the properties of graphene, the one that I find most interesting comes directly from the fact that it is a 2D crystal, that means each atom of it is available to image and modify. In an ideal case, one can attach a molecule between graphene electrodes and image it, get all the information about the binding configuration and conformational state of the molecule with respect to the 2D electrodes. One can on-purpose make defects in the crystal at predefined positions to modify the charge transport by scattering of electrons through those defects (See Chapter 5). Another benefit of 2D electrodes is that one could use the STM tip to gate the molecule very locally and it would also be possible to probe it using light. A 2D structure will also reduce the screening of the gate potential in comparison to the metallic electrodes, and produce negligible image charge effects.

### 7.3 Electromigration, electroburning vs direct cutting methods

Making nanogaps using electro-migration in metallic electrodes is not new and has been demonstrated as a useful technique to study single molecules<sup>[13–16]</sup>. Graphene

---

<sup>6</sup> It is reported that these amine groups form covalent amide bonds with graphene, which are strong enough to withstand many chemical treatments.

[4] Jan A. Mol et al. In: *Nanoscale* 7 (2015), p. 13181.

[5] Konrad Ullmann et al. In: *Nano Letters* 15 (2015), p. 3512.

[6] Yang Cao et al. In: *Angewandte Chemie* 124 (2012), p. 12394.

[7] Yang Cao et al. In: *Angewandte Chemie International Edition* 52 (2013), p. 3906.

[8] Jeong-Yuan Hwang et al. In: *Nanotechnology* 21 (2010), p. 465705.

[9] Florian Banhart et al. In: *ACS Nano* 5 (2011), p. 26.

[10] Hatéf Sadeghi et al. In: *Beilstein journal of nanotechnology* 6 (2015), p. 1413.

[11] Pascal Gehring et al. In: *Nano Letters* 17 (2017), p. 7055.

[12] V. M. García-Suárez et al. In: *Phys. Rev. B* 87 (2013), p. 235425.

[13] Hongkun Park et al. In: *Applied Physics Letters* 75 (1999), p. 301.

[14] Herre S. J. van der Zant et al. In: *Faraday Discuss.* 131 (2006), p. 347.

[15] Edgar A. Osorio et al. In: *Nano Letters* 7 (2007), p. 3336.

[16] Maria Rudneva et al. In: *Microscopy and Microanalysis* 19 (2013), p. 43.

### 7.3 Electromigration, electroburning vs direct cutting methods

---

electrodes on the other hand are mostly prepared using electroburning<sup>[3-5,11,17-28]</sup> techniques. Here, first a pre-patterned nano-ribbon or notch is made in the graphene using electron-beam lithography followed by oxygen plasma etching. The typical width of such a constriction is from 100 to 200 nm. For further narrowing down the notch, an electroburning process is used for which the presence of an oxygen environment is essential. In this process, at high current, a temperature activated reaction is started with the oxygen molecules striking the graphene lattice. This reaction removes the carbon atoms from the graphene lattice by oxidation. Due to highest current density the narrowest part of the junction gets heated most and burn. To add further control on the nanogap formation, a feedback loop is implemented. Here, first, the applied voltage across the pre-patterned junction is slowly increased (at a typical rate of 0.75 V/s to 1 V/s) with the feedback set to the measured current. Then as a drop in current is recorded, the voltage is ramped back to zero (at a typical rate from 0.225 mV/ $\mu$ s to 0.1 V/ $\mu$ s). This procedure is repeated until a tunnelling junction is formed, which is found mostly as having a resistance larger than 500 M $\Omega$ .

Just before the final breakdown to tunnelling, a sudden rise or peak in current in roughly 50 % of the junctions is reported. This mysterious peak was explained later<sup>[23]</sup> as a consequence of quantum interference with a crossover from multiple path connectivities of carbon atoms to single path connectivity. This is contradicted by another group<sup>[21,26]</sup> which claim to have not seen this peak in conductance and that there is a large chance of making uncontrollable gaps when the electro-burning is done in air. The same group<sup>[21,26]</sup> further claims to have achieved better control and large yield of nanogap formation while working in high-vacuum ( $10^{-7}$  mbar). They explain it as a sublimation process rather than an oxidation process as was the case in electroburning. Furthermore, the reason behind better control in high-vacuum is given based on the exothermic nature of the electroburning technique. Ullmann *et al.*<sup>[5]</sup> have performed also a similar high vacuum test (see their supplementary information) and reported no breakdown of the junction, rather emission of white light visible to the naked eye followed by a complete collapse of the structure. It is possible that the different substrates used in these experiments explains some of the differences in results.

Irrespective of the method used for making these graphene junctions, a large yield of formation (> 90 %) is claimed<sup>[3,21]</sup>. Important to note is that this yield does not

---

<sup>7</sup> IV measurements on single carbon atom chain<sup>[29]</sup> shows non-linear behaviour, but to a rough estimate for 150 mV it carries a current of 1 nA giving it a resistance of around 150 M $\Omega$ .

[17] Enrique Burzur *et al.* In: *Graphene* 1 (2012), p. 26.

[18] Amelia Barreiro *et al.* In: *Nano Letters* 12 (2012), p. 6096.

[19] J. O. Island *et al.* In: *Journal of Physics: Condensed Matter* 26 (2014), p. 474205.

[20] C. S. Lau *et al.* In: *Phys. Chem. Chem. Phys.* 16 (2014), p. 20398.

[21] Cornelia Nef *et al.* In: *Nanoscale* 6 (2014), p. 7249.

[22] Pawe Puczkarski *et al.* In: *Applied Physics Letters* 107 (2015), p. 133105.

[23] Hatef Sadeghi *et al.* In: *Proceedings of the National Academy of Sciences* 112 (2015), p. 2658.

[24] Pascal Gehring *et al.* In: *Nano Letters* 16 (2016), p. 4210.

[25] Chit Siong Lau *et al.* In: *Nano Letters* 16 (2016), p. 170.

[26] Maria El Abbassi *et al.* In: *Nanoscale* (2017), pp. -.

[27] Laszlo Posa *et al.* In: *Nano Letters* 0 (2017), null.

[28] Syed Ghazi Sarwat *et al.* In: *Nano Letters* 17 (2017), p. 3688.

mean that this high percentage of junctions are usable. Gehring *et al.*<sup>[11]</sup> reports that only 16 % showed successful signatures of molecule deposition, which also include multi-molecule junctions. The success rate is reduced by the numbers of junctions that break but have a larger gap between graphene electrodes, multiple molecules binding or small weakly connected ( $T < 0.5$ ) charging islands<sup>[3,20]</sup> left between the electrodes after electroburning. These islands can already give Coulomb blockade and Kondo signatures without any molecule deposition. Formation of similar islands is also seen in metallic junctions formed by electromigration in almost 30 % cases<sup>[14,30]</sup> and also in freestanding graphene<sup>[31]</sup>. A clear mechanism for the formation of these islands is not understood yet. It is believed that the formation of graphene quantum dots is due to electron-hole puddling or charge localisation, which could lead to the formation of these carbon islands as a leftover of electro-burning. In metallic junctions, this quantum dot formation was later avoided by using a self-breaking technique<sup>[32]</sup>, where once a few conductance quanta were achieved by the usual electromigration technique, the contact is left to break by room-temperature thermal diffusion by putting the bias to zero. The quantum dot formation in graphene is not resolved yet.

This is a reason why many groups prefer using multi-layer graphene and graphene grown on SiC<sup>[5]</sup> because on doing this the formation of charge puddling is less. Burzuri *et al.*<sup>[17]</sup> have shown by measuring success statistics that the electroburning procedure is more controlled in this multi-layer graphene as compared to single layer graphene. As a draw-back, in case of multilayer graphene, the layers on the bottom (close to the substrate) are burned later than the ones on top, and thus the minimum gap width is near the substrate, which makes it difficult to image them using SPM.

The only other method used for making graphene electrodes for molecular electronics applications is dash-line lithography (DLL) technique developed by Cao *et al.*<sup>[6,7,33]</sup>. In the DLL technique sub 5 nm nanogaps are made in single-layer graphene on SiO<sub>2</sub> substrate using a combination of e-beam lithography and oxygen plasma etching. They first covered the graphene with PMMA, a window in the PMMA is opened using e-beam, and then by utilizing the gradual etching and undercutting of PMMA when exposed to oxygen plasma they were able to make graphene point contacts with sub 5 nm gaps. Conventional O<sub>2</sub> plasma etching (which is also normally used for pre-patterning the constriction in graphene for electroburning) produces a large number of defects on the edges and leads to coverage of the edges by carboxylic acid end-groups. Huang *et al.*<sup>[34]</sup> discusses a neutral beam method for making ultra low edge-defect graphene nanoribbons. In the neutral beam etching technique, the charged ions were neutralised, and the UV photons are reflected back by use of graphite based grids.

Thiele *et al.*<sup>[35]</sup> have used helium ion milling to make nanogaps of around 3 nm in graphene nanotubes where the gap size was estimated by studying the secondary electrons intensity profile. They demonstrated suspension of a 3.9 nm long OPE

[30] A. A. Houck *et al.* In: *Nano Letters* 5 (2005), p. 1685.

[31] J. Moser and A. Bachtold. In: *Applied Physics Letters* 95 (2009), p. 173506.

[32] K. O'Neill *et al.* In: *Applied Physics Letters* 90 (2007), p. 133109.

[33] Huimin Wen *et al.* In: *Science Advances* 2 (2016).

[34] Chi-Hsien Huang *et al.* In: *Carbon* 61 (2013), p. 229.

[35] Cornelius Thiele *et al.* In: *Applied Physics Letters* 104 (2014), p. 103102.

## 7.3 Electromigration, electroburning vs direct cutting methods

---

molecule in this gap using phenanthrene anchor groups. Other methods to do nanopatterning on graphene over SiO<sub>2</sub> includes selective carbothermal etching<sup>[36]</sup>.

### 7.3.1 Estimation of nanogap size

The characterization of the width of the nanogap formed by electromigration or electroburning is difficult using direct measurement methods (like SEM/TEM/STM/AFM) and is commonly estimated by fitting the IV characteristics (or resistance) using the Simmons model<sup>[37,38]</sup>. Simmons' model can be used to calculate the current once a few free parameters are fixed: the gap width, the barrier height<sup>[3]</sup>, cross-section area of the junction and the asymmetry in the bias voltage response. Nef *et al.*<sup>[21]</sup> point out that the Simmons model fitting should be valid for smaller bias only where the tunnel barrier can still be approximated by trapezoidal barriers. At higher bias, the trapezoidal tunnel barriers changed to a triangular shape and the effective gap size reduces. The voltage at which transition from trapezoidal to triangular shape tunnel barriers occurs can be estimated from a Fowler-Nordheim plot, i.e. plotting  $\ln(1/V^2)$  vs  $1/V$ . However, the cross-section area of the junction is difficult to estimate, as there is no reason to assume the cut made by electroburning to form two parallel edges on the electrodes. Thus this value has to be adjusted by hand. Approximate values for the barrier height reported by different groups are around 0.24-0.5 eV which is much smaller than the work-function of graphite (around 5 eV). Moreover, in a recent article Posa *et al.*<sup>[27]</sup> have suggested that the substrate SiO<sub>x</sub> may also take part in the tunnelling process which would lead to a broad range of possible values for the barrier height.

### 7.3.2 Direct cutting methods

Other than the above techniques there are many direct cutting methods which have been used for making structures in graphene and have not yet been explored from a molecular electronics perspective for making graphene-based electrodes. By direct cutting methods, we mean methods are not based on the selection of the desired gap distance from many attempts but rather can be used to make controlled and desired patterns in graphene. These include, focussed He ion beam<sup>[35,39-42]</sup>, focused Ga ion beam<sup>[43]</sup>, catalytic reaction based chiseling<sup>[44]</sup>, and scanning probe microscopy tip induced cutting<sup>[45]</sup>, which includes AFM<sup>[46]</sup> and STM<sup>[47,48]</sup>. Some studies on

---

[36] Péter Nemes-Incze et al. In: *Nano Research* 3 (2010), p. 110.

[37] John G. Simmons. In: *Journal of Applied Physics* 34 (1963), p. 1793.

[38] Ayelet Vilan. In: *The Journal of Physical Chemistry C* 111 (2007), p. 4431.

[39] Braulio S. Archanjo et al. In: *Applied Physics Letters* 104 (2014), p. 193114.

[40] Ahmad N. Abbas et al. In: *ACS Nano* 8 (2014), p. 1538.

[41] D. C. Bell et al. In: *Nanotechnology* 20 (2009), p. 455301.

[42] Nima Kalhor et al. In: *Microelectronic Engineering* 114 (2014), p. 70.

[43] Hu Li et al. In: *Scientific reports* 6 (2016), p. 19719.

[44] Wei Li Wang et al. In: *Nano Letters* 14 (2014), p. 450.

[45] Pasqualantonio Pingue. In: *Tip-Based Nanofabrication*. Springer, 2011, p. 357.

[46] Péter Nemes-Incze et al. In: *Scientific Reports* 7 (2017).

[47] Levente Tapaszto et al. In: *Nature Nanotechnology* 3 (2008).

[48] Gabor Zsolt Magda et al. In: *Nature* 514 (2014).

free-standing graphene using high-resolution TEM have also been performed<sup>[49,50]</sup> showing cutting (via a TEM sculpting process) and imaging of nanometer size gaps. The focused ion beam and electron beam etching techniques have not been tested very well for the amount of damage to the graphene lattice they do near the cut edge. The only images of the cuts are from secondary electrons and do not have the high resolution needed to address that.

## 7.4 Our approach

We decided to explore a few of the direct cutting methods, to study their potential for making graphene-based electrodes. The techniques that we choose for our study are the helium ion milling technique and cutting by scanning probe microscope tip. The benefit of direct cutting methods is that one can have well-defined gaps between the two electrodes which makes it possible to characterize them with STM at the atomic scale and the possibility to scale up to a circuit with many molecular units.

### 7.4.1 Helium-ion milling

The He ion milling (HIM) technique was claimed to give more narrow cuts and lower damage than e-beam techniques due to a smaller de-Broglie wavelength of helium ions<sup>[51,52]</sup> as compared to electrons. However, the amount of damage that occurs in the graphene lattice close to areas etched by HIM has not been shown at the atomic scale. We are targeting these HIM cuts for separating electrodes and hanging molecules between them, so the characterisation of the structure of graphene close to the edges is important. For this study, we choose graphene on boron nitride (BN) as our sample. The choice of BN as the substrate has three benefits. Firstly, as BN has a crystalline structure (compared to commonly used amorphous SiO<sub>x</sub>) with lattice constant similar to that of graphene, the substrate corrugation is small which will make finding and imaging small cuts made by HIM easier. Secondly, BN is known to reduce charge puddling which increases the overall electron mobility of electrons. Thirdly, as BN forms a flat substrate for graphene with better lattice match, one can reduce the multiple scattering of secondary electrons, which is expected to reduce the damage near the etched area.

The graphene-BN sample was prepared in TU Delft with a multi-step wet transfer technique described by Dean *et al.*<sup>[53]</sup>. In this method, first the BN is exfoliated on a SiO<sub>2</sub> substrate while the graphene is exfoliated on a polymer stack consisting of PMMA and a water soluble layer. In the next step, the SiO<sub>2</sub> substrate is detached by floating the stack with graphene over a deionized water bath. After this the PMMA<sup>8</sup> with the monolayer graphene is clamped using a glass slide on a micro-manipulator. Then with the use of a modified optical microscope setup and an x,y,z micrometer

---

<sup>8</sup> The thickness of the PMMA is tuned to have a sufficient optical contrast for detection of the mono-layer graphene.

[49] Ye Lu et al. In: *Nano Letters* 11 (2011), p. 5184.

[50] Felix Bärnert et al. In: *ACS Nano* 6 (2012), p. 10327.

[51] John Notte et al. In: *AIP Conference Proceedings* 931 (2007), p. 489.

[52] Max C. Lemme et al. In: *ACS Nano* 3 (2009), p. 2674.

[53] Cory R. Dean et al. In: *Nature nanotechnology* 5 (2010), p. 722.

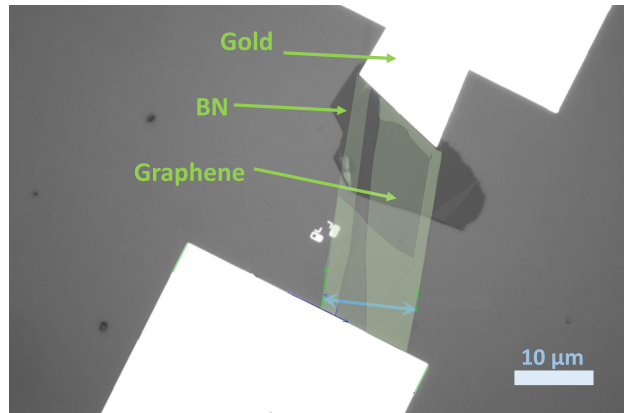


Figure 7.1: Graphene-BN sample prepared at TU Delft using the method described by Dean *et al.*<sup>[53]</sup>.

stage, one can align the monolayer graphene over the multi-layer BN flake. Then by stamping graphene over BN and later dissolving the PMMA using acetone, one can transfer the graphene over the BN. An optical image of the sample is shown in Figure 7.1. Then Helium ion milling is used to make cuts in this graphene-BN sample using different ion doses (from  $1 \times 10^{16}$  to  $8 \times 10^{16}$  ions/cm<sup>2</sup>).

The next task is to approach the STM tip on this small sample for imaging. Just to remind, the sample is prepared by exfoliation and so the size of such samples are of the order of a few tens of microns. Two methods were followed from here: first, an ambient JPK STM<sup>9</sup> was modified by use of an optical microscope to guide the STM tip to the small graphene flake. Second, for our UHV STM due to size constraint, it is not possible to mount an optical camera with sufficient resolution, which could guide the tip to the graphene flake. So, a capacitive sensing technique was implemented here. This is described in detail in the master thesis of Kim Akius<sup>[54]</sup>. A brief account is first given of the capacitive technique and then we will look into the helium ion beam induced cuts.

### Capacitive scanning technique

The idea is to use the capacitance of the tip-sample system to navigate to the graphene flake, while avoiding the risk of crashing the tip on the non-conducting SiO<sub>2</sub> surface surrounding the graphene sample. The capacitance has an approximate  $1/z$  dependence on distance between tip and sample which makes it more suitable for approach from large distance than the exponentially decaying tunneling current. Another fact that we use here is that the gradient of the measured capacitance signal with distance  $dC/dz$  is directly proportional to the gradient of the electric field  $dE/dz$ . By putting an equal and opposite bias voltage on the sample (i. e. graphene and gold pads) and the back gate (i. e. the highly doped Si substrate), one can enhance the electric field gradient (and thus the gradient of the capacitively measured signal) at the edges of

---

<sup>9</sup> <https://www.jpk.com/>

[54] Kim Akius, Master thesis, Leiden Institute of Physics (LION), Leiden University. 2015.

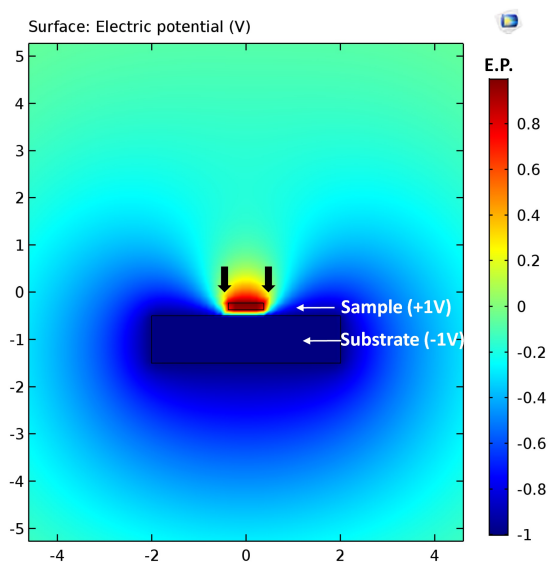


Figure 7.2: COMSOL Multi-physics output of an electric potential surface showing large gradients at edges marked by black arrows. The substrate (dark blue) is put at a potential of -1 V, while the sample (red) is put at 1 V. The color scale at the right encodes for the strength of the local electric potential.

the conductor (as shown in Figure 7.2). By combining these two ideas and by measuring the large electric field gradient one can image the boundaries of the gold leads that guide us to graphene by scanning at a distance of few microns above the surface. Figure 7.3(a) shows the capacitive image of the sample with the inset showing the corresponding optical image. The capacitive image shown here is a low-pixel image with only a small number of line scans, just to show the proof of concept that the implementation works. For landing on the graphene flake, we used a more direct method which we call the ‘saddle point method’ which will work for the symmetric leads geometry like ours. Here we first make two parallel line scans along the x-axis (AB, CD shown in the inset of Figure 7.3(a)). Then connecting the peak positions in AB and CD line scans, we define a new scan direction EF. The minimum in the capacitance measurement along this line gives the position of graphene. One can do a last check again along the line GH (parallel to AB or CD) if needed. Figure 7.3(b) shows an atomic resolution image we obtained after landing the STM tip into tunneling distance on graphene.

For the above test, we used a sample without HIM cuts. For our sample with HIM cuts, we decided to test it first in the ambient JPK STM. For this, as mentioned before, we used an optical microscope and mechanically etched tip to navigate to the micrometre size graphene sample. We also used a map of the surface topography and cuts made before by an ambient AFM measurement for navigation. Figure 7.4 (a) and (b) shows the HIM cuts in height and phase AFM image. This AFM map was essential as we want to keep the fast scan direction in STM mode perpendicular to the cut axis. This is to minimize the risk of tip crashes when the tip moves over

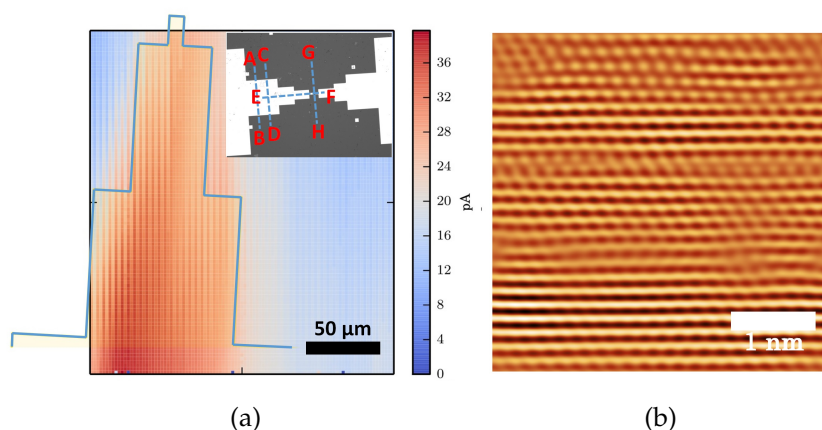


Figure 7.3: (a) Image of the gold electrode using the capacitive scan (b) Atomic resolution using STM after approaching on the small patch of exfoliated graphene.

the cut as the BN substrate is an insulator. After this, we approached with the STM, but on scanning with STM, we found that there was a lot of contamination deposited close to the cuts. A line profile crossing all the cuts is shown in Figure 7.4 (c). The contamination could be due to bad vacuum in the HIM setup, which causes carbon deposit due to activation by the helium ions themselves. Unfortunately, we could not make another attempt with better vacuum due to technical problems in the HIM setup in TU Delft. However, it will be important in future to further explore cuts made on graphene using HIM and other FIB techniques.

With this experience we started to look for less intrusive techniques like SPM tip cutting techniques where the damage is very local and less sensitive to the cleanliness of the environment, so that there is minimal to no damage close to the place where the cut is made.

#### 7.4.2 Scanning probe microscopy based cutting

The main benefit of cuts made by tips of atomic force microscope and scanning tunnelling microscopes is that there will be hardly any damage on the graphene lattice near the cut. We started by exploring the parameters for cuts made using atomic force microscope tips. This turned out to be a less promising approach because while attempting making smaller cuts we suspect we are creating local strains in the graphene rather than cutting through it. This is due to strong  $sp^2$  bonds and high flexibility of the graphene lattice<sup>[46]</sup>.

Scanning tunnelling microscope based cutting of graphene seems a better option to make smaller cuts. It needs to be made not by dragging the tip over the graphene surface as in AFM but rather by the localized breaking of bonds due to high field gradient between tip and sample. Although it shares some similarity with the electroburning technique, there are also marked differences between the two. In electroburning, a large cross-section (from 100 to 400 nm wide) of graphene is heated and partly burned, and the profile of the cut is not uniform or parallel. Here, in STM based cutting uniform parallel edges can be formed. Further, as the cuts are made

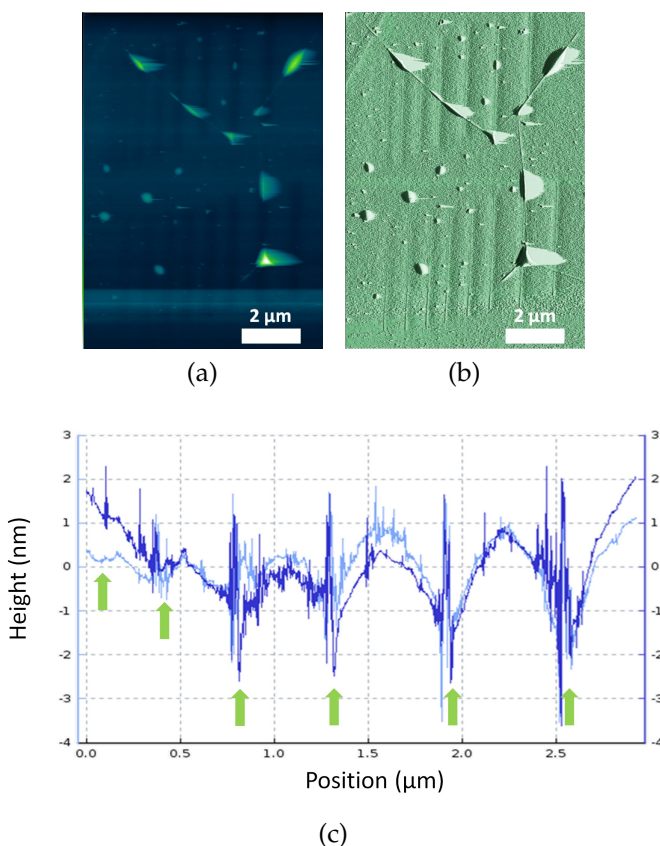


Figure 7.4: (a) AFM height image of a graphene sample on top of BN showing He ion beam induced cuts for doses ranging from  $1 \times 10^{16}$  to  $8 \times 10^{16}$  ions/cm<sup>2</sup>. (b) Phase image using AFM of the same area. (c) Topography line profile crossing all the cuts using STM shows lot of contamination deposited close to the cut regions (marked by green arrows).

by moving the STM tip over the surface, any desired pattern can be cut into the graphene, which makes it very easy to shape multiple electrodes.

Such type of STM based cutting of graphene layers and graphite has been demonstrated earlier by many groups<sup>[47,48,55,56]</sup>. Albrecht et al.<sup>[55]</sup> in 1989 have shown a procedure for making cuts in graphite. They have tested it in air, vacuum, O<sub>2</sub>, N<sub>2</sub>, water, benzene and in water vapour environment. They report that the cut happens only in air and also in the presence of a mild partial pressure of water vapour (such as a vapour pressure of 25 mbar) but have not seen any cut formation in vacuum below 13 mbar and not in oxygen or nitrogen environment nor in pure water and benzene environment. They claim that the cutting cannot be a mechanical effect and further

[55] T. R. Albrecht et al. In: *Applied Physics Letters* 55 (1989), p. 1727.

[56] Hidefumi Hiura. In: *Applied Surface Science* 222 (2004), p. 374.

claim that water is important for cutting. A chemical reaction induced by the pulse may be responsible for cutting. Similar results with better control over the cleanliness of the cuts have been shown later by Kondo *et al.*<sup>[57]</sup>, Hiura<sup>[56]</sup> and Tapasztó *et al.*<sup>[47]</sup> who have used it for making graphene nanoribbons. Magda *et al.*<sup>[48]</sup> have used this method to make nano-ribbons in graphene transferred onto a Au surface. In contrast to the work by Albrecht *et al.*<sup>[55]</sup>, Kondo *et al.*<sup>[57]</sup> have shown that cuts in graphite can also be made in UHV which takes place via sublimation at higher bias.

### Study of the mechanism behind STM cutting

Important to note is that the mechanism proposed for this cutting technique suggests that a water layer on top of the graphene is essential. This is interesting because the electroburning of graphene is also performed mostly in ambient conditions, but the oxidation of graphene there is supposed to be initiated by oxygen in the environment rather than water layer on the surface. The close proximity of the STM tip to the surface may limit the number of oxygen molecules striking the region below the tip, and the cutting by the STM tip does not result from burning due to poor heat transport to the bulk but is rather a chemical reaction in the presence of water. Using the STM based localized cutting technique for graphene placed on insulating substrates will be an interesting test of the mechanism. One can further test this STM based cutting over pre-patterned graphene nanoribbons, where heat transport to the banks is also reduced.

To show the potential of this technique, I present sub 5 nm clean, controlled cuts (Figure 7.5) made into the top graphene layer on graphite using an STM tip. The parameters used here were 2.8 V bias, 6 nA tunnel current, 5 nm/sec tip speed. Very few attempts have been made in the past in this direction due to the exponential dependence of the tunnelling current. On cutting the layer below the tip, the size of the vacuum gap changes which reduces the tunnelling current abruptly and the feedback control loop could start to rattle<sup>[45]</sup>. Further, this could also lead to a tip crash when there is only one layer of graphene and an insulator below it. So before we start with graphene on an insulating substrate, we need to get the process under control and the parameter space properly tested.

I will discuss now in detail, the effect of different parameters (tunnelling current, bias, and tip speed) and try to understand the cutting mechanism at the atomic scale<sup>10</sup>. We will also show a time evolution study of the cut. For this, we test bias values from 2.6 V to 2.9 V and tunnelling currents from 500 pA to 1.5 nA, by making a 10×10 grid as shown in Figure 7.6. Here, instead of making line cuts, we decided to test the parameters by making pits or holes into the top graphene layer. So, instead of the tip speed, we kept a fixed tip hold time<sup>11</sup> of 2 seconds while fixing the position of the STM tip. We see in Figure 7.6, that the cuts are less sensitive to the tunnelling current than to the bias voltage. As the reaction in the presence of water is endothermic, high tunnel currents could increase the reaction rate. However, the magnitude of tunnel current we are working with will generate a very small amount of heat and thus it

---

<sup>10</sup> This work is done together with Kim Akius, PhD student in our group.

<sup>11</sup> Hold time is a time-period in which the STM tip is kept at a particular (x,y) position above the graphene layer (at a tunnel gap) where the cut is supposed to be made.

[57] Seiichi Kondo *et al.* In: *Applied Surface Science* 75 (1994), p. 39.

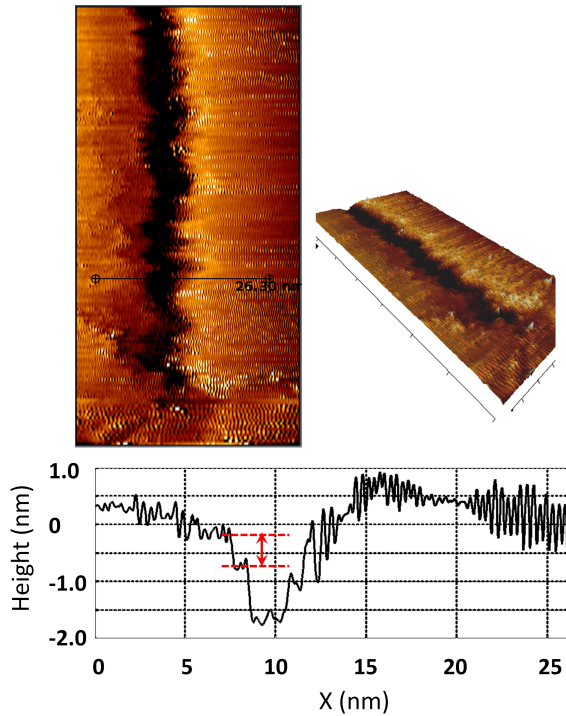


Figure 7.5: Sub 5 nm cut made using STM tip manipulation. A layer step height is marked with the red arrow.

may not increase the local temperature more than 5 deg<sup>[56]</sup>, so the effect of the tunnel current is estimated to be minimal.

Next, we fixed the tunnel current value to 500 pA and bias to 2.85 V and we performed a scan over the hold time (from 10 ms to 1 sec). Figure 7.7 shows, how the cut topography changes for different hold times. The procedure starts at the bottom-left corner with 10 ms hold time and ends at the top-right corner with 1 sec hold time. The hold time is always increased (with equal steps) moving up in each column. This is in fact, a time evolution of the cut for a particular bias and tunnel current value. What we see in this time evolution is that at the earlier stages of the cut, the top layer graphene seems to be only deformed, while as the time evolves, at some point cuts start to appear.

To understand the process further, we need to examine the sequence of operations performed. The procedure used for cutting is— first change the tunnel current setpoint to 500 pA while keeping the bias at 100 mV, this moves the tip closer to the surface. Until this point, there will be no cut as the bias is very small. Next, we slow down the feedback, to avoid rattling of the STM tip. Then we set the bias to the desired value of 2.85 V with a ramp speed of 10 V/s. Due to slow feedback, the STM tip slowly moves away from the surface. Such a procedure lifts locally the top layer graphene with the tip due to electrostatic forces. This breathing mode of graphene has been reported

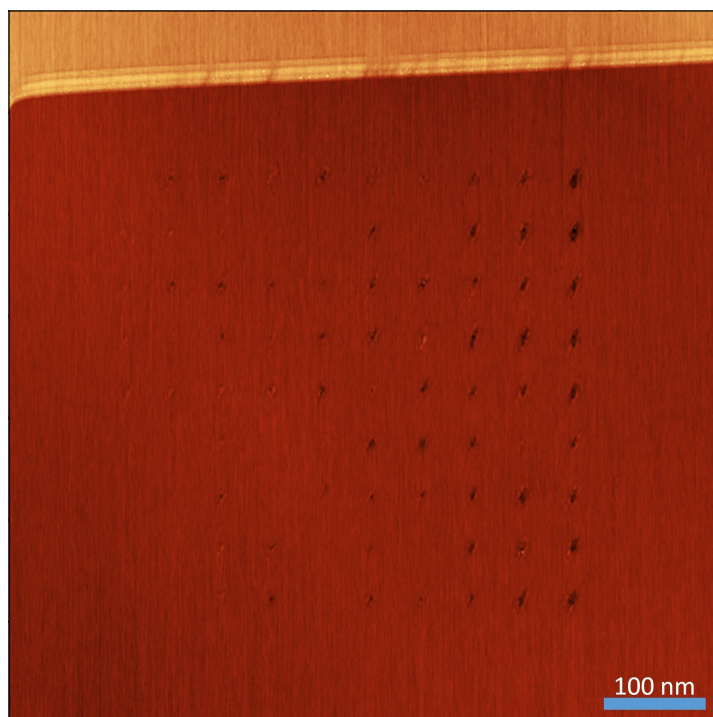


Figure 7.6: Parameter space study of STM current and voltage controlled cutting: In this 10×10 grid the tip-sample bias is increase from 2.6 V to 2.9 V with equal steps in the horizontal direction from left to right, so each column corresponds to one bias value. The tunneling current setpoints are increased from 0.5 nA to 1.5 nA in the vertical direction from bottom to top. Each point is spatially separated by a distance of 50 nm in the horizontal and vertical direction.

earlier<sup>[58,59]</sup>. As the tip is pulled up by the feedback, the bias is also increasing. The hold time is measured from the moment the bias is set by the software. Figure 7.8 shows an STM image of such a lift of the top layer graphene.

At the same time during this feedback-controlled lifting the bias continues to increase, which can create sufficiently large field gradients to initiate reactions with the layer of water on top of graphene. This reaction of carbon with water can remove carbon from the graphene by forming CO and H<sub>2</sub> gases<sup>[47,56,57]</sup> as products. Lifting of the top layer of graphene due to electrostatic forces can also break C-C bonds in graphene<sup>[60]</sup> by stretching. This was shown under ultra-high vacuum conditions where the presence of water on the surface can be neglected. This means that the cut in the top layer graphene that we see at the end can also be occurring due to the strain caused by the STM tip.

In either case, by controlled selection of parameters, we could attain cuts with

[58] Hong Seng Wong et al. In: *ACS Nano* 3 (2009), p. 3455.

[59] P. Xu et al. In: *Phys. Rev. B* 86 (2012), p. 085428.

[60] C. Rubio-Verdu et al. In: *Phys. Chem. Chem. Phys.* 19 (2017), p. 8061.

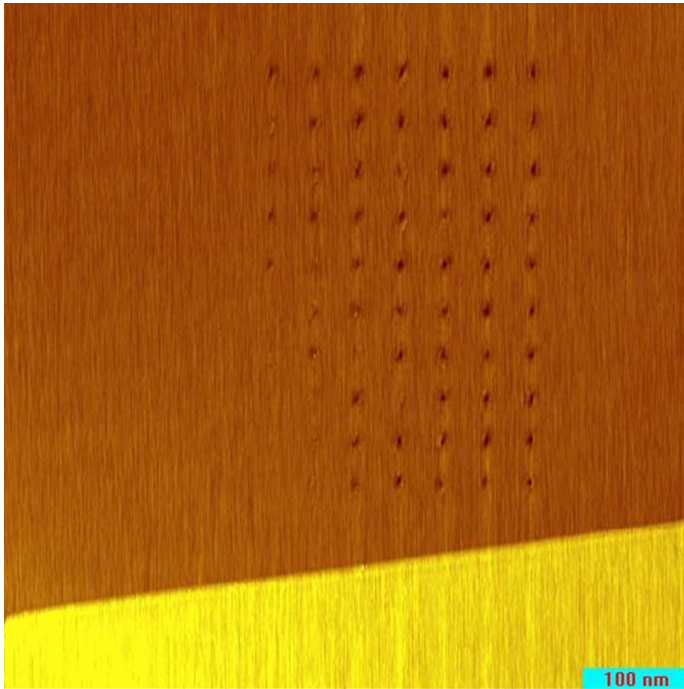


Figure 7.7: Time evolution study of the cut: In this  $10 \times 10$  grid the tip-sample bias and tunneling current setpoint are fixed at 2.85 V and 500 pA. The hold time is increased with equal steps between 10 ms to 1 sec. Each point is spatially separated by a distance of 50 nm in the horizontal and vertical direction.

the full width half maximum (FWHM) of around 1.61 nm as shown in Figure 7.9. As the cuts happen while the top-layer graphene is isolated from the bulk graphite, we think this technique should be easily applicable to make controlled cuts on graphene over an insulator.

## 7.5 Conclusion

We have demonstrated the potential of STM based technique for making controlled nano-gaps into the top-layer of graphene over graphite. This technique holds strong similarities with the commonly used electro-burning technique with an added advantage that here the burning due to oxidation or sublimation (under UHV)<sup>[57]</sup> can be done locally and with better control. This STM based technique needs to be developed further and applied to graphene over an insulator. In order to decide whether the cutting of the top layer graphene shown here is because of strain induced by electrostatic forces or oxidation due to the presence of water or both, we need to repeat the experiments by changing the order of operations. In the experiments described above, we first define the setpoint tunnel current and tuned the feedback slow. Following this we ramped the bias to the desired value. This made the STM tip to first come close to the surface and then retract pulling with it the top graphene layer. Another procedure to do this is to start by first retracting the tip a couple

## 7.5 Conclusion

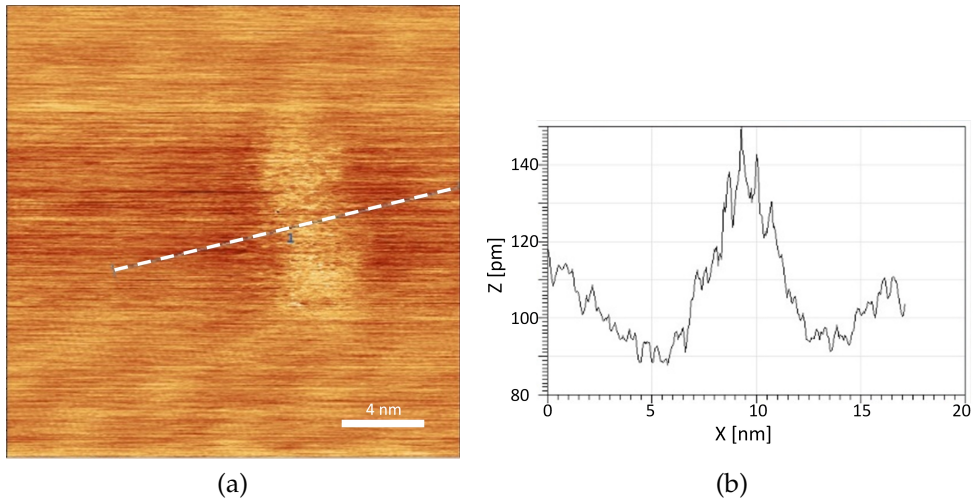


Figure 7.8: (a) A hump formation due to pull out of a single layer graphene at early stages (49.6 ms hold time) of the cut with 500 pA tunnel current and 2.85 V bias. (b) Line profile made along the white line.

of nanometers above the scanning position and slowing down the feedback. Then change to the desired tunnel current setpoint and begin ramping the bias. This will make the STM tip to move only closer to the surface until the height corresponding to the set tunnel current and bias is achieved. This will avoid lifting of the top layer.

Alternatively, one could match the speed of tip retraction and the rate of bias change such that the field gradient is kept constant throughout. By doing this, the cut (if any) will only be formed because of tip-induced electrostatic pulling of the top graphene layer. However, the cuts where multiple graphene layers are cut using STM tip induced manipulation are more likely due to oxidation.

For cuts to be made in graphene over an insulator using STM tips, we need to implement a custom feedback loop. As we cut the part of graphene below the tip, the tunnel current will decrease, and the standard feedback will bring the tip closer looking for the desired setpoint. This is also what happens in graphite, but there the tip on coming closer by one atomic layer distance starts to tunnel into the layer below and ideally stops there until new water molecules arrive or the operation is aborted when the hold time is finished. In graphene on an insulator, as there is no conducting layer beneath, the STM tip will come to the surface until the setpoint tunnel current is achieved by tunneling from the side of the etched region. On arriving at this point, the cutting may continue through the sides as there is water all over the graphene. This may thus lead to crashing of the tip to the insulator. A custom-made feedback system with a predefined cut-off limiting the  $z$  displacement to less than one atomic layer height can be implemented.

A first application of this method would be the possibility of making more than two electrodes on a molecular junction using the STM cutting technique, in the form of a side-gate. Puczkarski et al.<sup>[22]</sup> have demonstrated the fabrication of a three-terminal single electron transistor (SET) using graphene electrodes with a side gate using the electroburning technique. They claim a three-fold increase in gate coupling

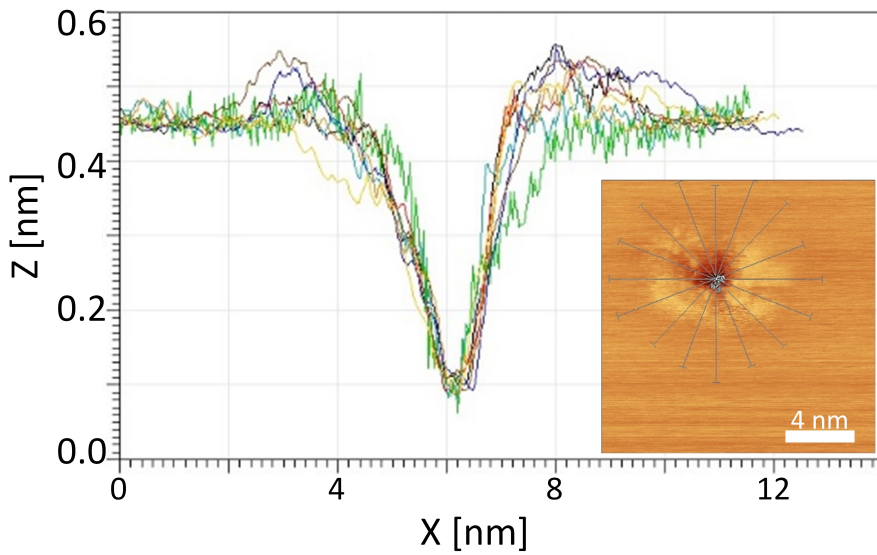


Figure 7.9: Line scans over a cut made with optimized parameters shows a full width half maximum (FWHM) of 1.61 nm with depth of one layer of graphene. Inset shows the corresponding STM image.

in comparison to the conventional back-gate technique and further claim a gap size of several nanometers as obtained from a Simmons fit.